Analysis of Predetection Diversity TCM-MPSK and Postdetection Diversity TCM-MDPSK Systems on a Rayleigh Fading Channel

Guillem Femenias, *Member, IEEE,* and Ramon Agustí, *Member,IEEE*

Abstract – **In this paper, the bit error rate (BER) performance of predetection diversity trellis coded multilevel phase shift keying (TCM-MPSK) and postdetection diversity trellis coded multilevel differential phase shift keying (TCM-MDPSK), transmitted over a Rayleigh fading channel is presented. Novel analytical upper bounds using the transfer function bounding technique are obtained and illustrated by several numerical examples. A new asymptotically tight upper bound for the Maximal Ratio Combining (MRC) diversity schemes is also derived. In order to analyze practical TCM schemes (four or more states), only trellis codes holding uniform error property (UEP) and uniform distance property (UDP) are considered, enabling the encoder transfer function to be obtained from a modified state transition diagram, having no more states than the encoder itself. Monte-Carlo simulation results, which are more indicative of the exact system performance, are also given.**

I. Introduction

In recent years there has been an increasing interest in digital transmission in the field of mobile radio. The mobile radio channel is a multipath propagation medium, and hence if a relatively low bit rate signal with a bandwidth much smaller than the coherence bandwidth of the multipath channel is transmitted, signal envelope variation (multiplicative fading) and random FM noise will produce high error rates even with high average signal to noise ratios and place a lower limit on the achievable bit error rate (BER). One of the most efficient techniques to reduce fading effects is space diversity reception, in which several signals received on different antennas are combined [1], [2]. Another attractive technique is forward error correction (FEC) coding. Trellis coded modulation (TCM), originally developed for additive white Gaussian noise (AWGN), combined with interleaving, is known to have a powerful error correction capability in fading channels. Furthermore, the coding gain relative to the uncoded systems is available without extra bandwidth requirements and with simple decoders using the Viterbi algorithm. This property makes it suitable for transmitting digital sequences over bandlimited channels. Although previous papers [3]-[6] have been devoted to the BER performance analysis of TCM schemes on mobile fading channels, no analysis has been so far reported for their BER performance taking space diversity into consideration.

This paper investigates the BER performances of predetection diversity trellis coded MPSK (TCM-MPSK) and postdetection diversity trellis coded MDPSK (TCM-MDPSK), over a Rayleigh fading channel. The results are obtained by using a combination of theoretical analysis and simulation. In performing the analysis a number of simplifying assumptions are made. First, a theoretically ideal block interleaving/deinterleaving of channel signal is assumed in order that the channel may be considered as memoryless. This assumption leads to independent fading of the adjacent demodulated symbols and allows for considerable simplification of the analysis. Second, it is also assumed that fading over one baud interval may be represented by a single fading amplitude (slow fading approximation). Third, it is assumed that for TCM-MPSK systems the effect of the fading on the phase of the received signal is fully compensated for at the receiver and that for TCM-MDPSK systems the effect of frequency offsets between transmitter and receiver local oscillators is fully compensated for by tracking it with an ideal automatic frequency control (AFC). Thus, our results will address the degradation due to the effect of the fading on the amplitude of the received signal. Finally, although all simulation results reflect a finite decoding delay of six times the convolutional encoder constraint length, an infinite decoding delay is assumed in the analysis of the Viterbi decoding process.

The paper is organized as follows. The system and analysis models are presented in Section II. Section III contains the derivations of the average bit error rates for both predetection diversity coherent systems (TCM-MPSK) and postdetection diversity incoherent systems (TCM-MDPSK), considering a trellis decoder implemented as a Viterbi algorithm with a metric depending upon whether or not channel state information is available. In Section IV, an improved asymptotically tight upper bound for the Maximal Ratio Combining (MRC) diversity schemes is derived. Finally, discussion and conclusions are presented in Section V.

II. System and Analysis Models

The baseband system model under investigation is illustrated by the block diagram in Fig. 1. The elements indicated in dashed lines represent system functions that are peculiar to the form of detection, i.e., coherent versus differentially coherent. Input bits (representing data or digitally

Paper approved by Michel J. Joindot, the Editor for Radio Communications of the IEEE Communications Society. Manuscript received: April 27, 1992; revised June 9, 1993, August 24, 1993, and September 28, 1993. This work was supported by CICYT (Spain) under Grant TIC 880543.

G. Femenias was with the Departament de Teoria del Senyal i Comunicacions, Universitat Politècnica de Catalunya (UPC), Apdo. 30.002, 08080 Barcelona, Spain. He is now with the Departament de Ciències Matemàtiques i Informàtica, Universitat de les Illes Balears (UIB), E-07071 Palma de Mallorca (Balears), Spain.

R. Agustí is with the Departament de Teoria del Senyal i Comunicacions, Universitat Politècnica de Catalunya (UPC), Apdo. 30.002, 08080 Barcelona, Spain.

IEEE Log Number 9410070.

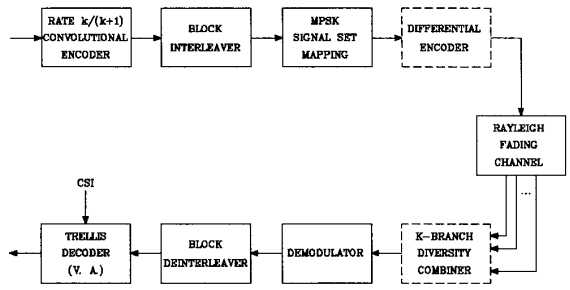

Fig. 1. Baseband system model.

encoded speech) at rate R_b are encoded by a rate $k/(k+1)$ trellis encoder producing an encoded symbol stream at rate $[(k+1)/k]R_b$. Trellis coded symbols (groups of $k+1$ bits) are next block interleaved to *randomize* the distribution of symbols affected by amplitude fading of duration greater than one symbol period and mapped, according to the *mapping by set partitioning rules* [7], onto an MPSK or MDPSK ($M = 2^{k+1}$) channel signal set. Transmitted signal is faded and corrupted by AWGN passing through the fading channel. At the receiver, in-phase and quadrature components are combined, demodulated, quantized for soft decision and block deinterleaved. Using these quantized symbols, the Viterbi decoder detects the transmitted sequence based on maximum likelihood estimation. Filtering is assumed to be of Nyquist type, equally split between emitter and receiver.

For a received sequence of length N, $Y_N=(y_1,...,y_N)$, the metric between Y_N and any transmitted signal sequence $X_N=(x_1,...,x_N)$, is of the form $m(Y_N, X_N; Z_N)$ if side information is available and $m(Y_N, X_N)$ if it is not. The metric is used by the decoder to make decisions as to which sequence was transmitted given the corresponding channel output sequences. Whatever metric is selected, to simplify the decoder processing complexity, it is required to have an additive property, i.e.,

$$m(Y_N, X_N; Z_N) = \sum_{n=1}^{N} m(y_n, x_n; z_n) . \tag{1}$$

Letting $m(Y_N, X_N; Z_N)$ denote the coding decision metric, the decoder incorrectly decides that the transmitted coded sequence is $\hat{X}_N \neq X_N$ when

$$m(Y_N, X_N; Z_N) \leq m(Y_N, \hat{X}_N; Z_N) , \tag{2}$$

with a probability $P(X_N \rightarrow \hat{X}_N)$ which is called the *pairwise error probability*. By our previous assumptions

$$\begin{aligned} P(X_N \rightarrow \hat{X}_N) &= Pr\left(m(Y_N, \hat{X}_N; Z_n) \geq m(Y_N, X_N; Z_N) \mid X_N\right) \\ &= Pr(f \geq 0 \mid X_N) \end{aligned} \tag{3}$$

where

$$f = m(Y_N, \hat{X}_N; Z_N) - m(Y_N, X_N; Z_N) . \tag{4}$$

An upper bound on the average bit error probability is obtained from $P(X_N \rightarrow \hat{X}_N)$ as [8]

$$P_b \leq \sum_{N=L_s}^{\infty} \sum_{X_N} \sum_{\hat{X}_N} a(X_N, \hat{X}_N)\, p(X_N)\, P(X_N \rightarrow \hat{X}_N) \tag{5}$$

where $a(X_N,\hat{X}_N)$ is the number of bit errors occurring when X_N is transmitted and $\hat{X}_N$ is chosen by the decoder, $p(X_N)$ is the *a priori* probability of transmitting X_N and L_s is the length of the shortest error event. If in one way or another the pairwise error probability can be expressed in product form, i.e.,

$$P(X_N \rightarrow \hat{X}_N) = \vartheta \prod_{n=1}^{N} W(x_n, \hat{x}_n) \tag{6}$$

with ϑ being a constant, then

$$P_b \leq \sum_{N=L_s}^{\infty} \sum_{X_N} \sum_{\hat{X}_N} a(X_N, \hat{X}_N)\, P(X_N)\, \vartheta \prod_{n=1}^{N} W(x_n, \hat{x}_n) \tag{7}$$

and the *pair state generalized transfer function bound* approach presented in [9] could be used for evaluating the average bit error probability bound just described. In fact, by labelling each branch between pair states in the transition diagram with a gain G of the form

$$G = \sum_{x_n} \sum_{\hat{x}_n} \frac{1}{2^k} Z^{a(x_n, \hat{x}_n)}\, W(x_n, \hat{x}_n) , \tag{8}$$

where the summations account for the possibility of parallel paths between pair-states in the trellis diagram, expression (7) reduces to

$$P_b \leq \frac{\vartheta}{kN_s} \left. \frac{\partial T(Z)}{\partial Z} \right|_{Z=1} \tag{9}$$

where $T(Z)$ denotes the transfer function of the pair-state transition diagram and N_s is the number of states of the trellis encoder. This approach, which has a complexity proportional to the square of the number of encoder states, is not considered practical for analyzing trellis encoder structures with more than two states. However, if the codes hold the Uniform Error Property (UEP) and the Uniform Distance Property (UDP) discussed in [10], without loss of generality, any transmitted sequence X_N can be chosen. In this case, a more efficient procedure (complexity proportional to the number of encoder states) for evaluating expression (7) is the *modified state transition diagram transfer function bound* approach proposed in [11]. In fact, by labelling each transition between states in the modified state transition diagram with a gain G of the form

$$G = \sum_{\hat{x}_n} Z^{a(x_n, \hat{x}_n)}\, W(x_n, \hat{x}_n) , \tag{10}$$

the average error probability upper bound can be expressed as

$$P_b \leq \frac{\vartheta}{k} \left. \frac{\partial T(Z)}{\partial Z} \right|_{Z=1} \tag{11}$$

where $T(Z)$ denotes the transfer function of the modified state transition diagram.

Taking into account that any trellis encoder consists of a linear binary convolutional encoder followed by a memoryless set of channel symbol assignments, determination of the encoder transfer function now requires specification of the binary convolutional encoder used at the transmitter. In this paper, only trellis codes holding UEP and UDP are considered. In particular, the rate 2/3 eight-state Ungerboeck's code [7], implemented by means of a systematic encoder with feedback is analyzed.

III. Average Bit Error Probability Bounds

A. Predetection diversity coherent systems (TCM-MPSK)

In phasor notation the nth element of the coded symbol sequence X_N, namely x_n, can be written as

$$x_n = \sqrt{2E_s}\, e^{j\Phi_n} \tag{12}$$

where $E_s = kE_b$ is the energy per MPSK symbol. The transmitted bandpass signal is

$$x_T(t) = \mathbf{Re}\left\{x(t)\, e^{j\omega_c t}\right\} = \mathbf{Re}\left\{\sum_k x_k\, h_T(t-kT)\, e^{j\omega_c t}\right\} \tag{13}$$

where ω_c is the carrier angular frequency, $h_T(t)$ represents the impulse response of the transmission filter and T is the symbol period.

Assuming, in general, a K branch diversity system, the complex envelope of the received signal on the kth receiver (k=1, 2, ..., K) can be expressed as

$$r_k(t) = \chi_k(t)\, x(t) + \nu_k(t) \tag{14}$$

where $\nu_k(t)$, which represents the additive thermal noise at the receiver front-end, is a zero-mean complex Gaussian noise process with single-sided power spectral density N_0 and

$$\chi_k(t) = \rho_k(t) \exp\left[j\psi_k(t)\right] \tag{15}$$

which represents the multiplicative Rayleigh fading characteristic of the channel, is a normalized (unit mean-square value), stationary, zero-mean complex Gaussian process. If the antenna spacing has been chosen so that the individual signals are uncorrelated then, each of the K antennas in the diversity array will provide an independent signal to the K-branch diversity combiner. A variety of techniques are available to perform the combining process and to capitalize on the uncorrelated fading exhibited by the K antennas in the space-diversity array [1], [2]. In *maximal ratio combining* (MRC) the K signals, after being cophased, are weighted proportionally to their signal voltage to noise power ratios and then summed. It is known that MRC provides the maximum possible improvement that a diversity system can attain through a fading channel. It may not always be convenient or possible to provide the adaptive weighting capability required for true maximal ratio combining. Instead, the gains may all be set equal to unity, and *equal-gain combining* (EGC) results. Finally, if the combiner connects to the output the receiver having the highest baseband signal-to-noise ratio, *selection diversity combining* (SC) results. Thus, the signal at the output of the combiner will be given by

$$g(t) = \sum_{k=1}^{K} \left[\rho_k^2(t)\, x(t) + \chi_k^*(t)\, \nu_k(t)\right] \quad (MRC) \tag{16}$$

$$g(t) = \sum_{k=1}^{K} \left[\rho_k(t)\, x(t) + e^{-j\psi_k(t)}\, \nu_k(t)\right] \quad (EGC) \tag{17}$$

$$g(t) = \rho_k(t)\, x(t) + e^{-j\psi_k(t)}\, \nu_k(t) \quad (SC)\,. \tag{18}$$
$$\rho_k(t) > \rho_q(t) \quad \forall\, q \neq k,\ q \in [1, .., K]$$

Then, the signal received at the output of the reception filter, $h_R(t)$, can be expressed as

$$w(t) = \sum_{k=1}^{K} \left[\sum_l x_l\, \rho_k^2(t)\, h(t-lT) + \chi_k^*(t)\, n_k(t)\right] \quad (MRC) \tag{19}$$

$$w(t) = \sum_{k=1}^{K} \left[\sum_l x_l\, \rho_k(t)\, h(t-lT) + e^{-j\psi_k(t)}\, n_k(t)\right] \quad (EGC) \tag{20}$$

$$w(t) = \sum_l x_l\, \rho_k(t)\, h(t-lT) + e^{-j\psi_k(t)}\, n_k(t) \quad (SC) \tag{21}$$

where $h(t) = h_T(t) * h_R(t)$ represents the overall impulse response of the system for a perfect non selective transmission medium and $n_k(t)$ is a filtered complex Gaussian noise process.

The signal at the output of the reception filter is sampled by an A/D converter at time $t_n = nT + \tau$, where $-T/2 \le \tau \le T/2$ determines the sampling instant. Assuming a perfect clock recovery, $\tau = 0$, the complex sample at the output of the deinterleaver will be given by

$$y_n = \sum_{k=1}^{K} \left[\rho_{k,n}^2 \sqrt{2E_s}\, e^{j\Phi_n} + \chi_{k,n}^*\, n_{k,n}\right] \quad (MRC) \tag{22}$$

$$y_n = \sum_{k=1}^{K} \left[\rho_{k,n} \sqrt{2E_s}\, e^{j\Phi_n} + e^{-j\psi_{k,n}}\, n_{k,n}\right] \quad (EGC) \tag{23}$$

$$y_n = \rho_{k,n} \sqrt{2E_s}\, e^{j\Phi_n} + e^{-j\psi_{k,n}}\, n_{k,n} \quad (SC)\,, \tag{24}$$

where, for simplicity of notation, we have dropped the delay introduced by the interleaving/deinterleaving process.

1) Ideal Channel State Information: The assumption of ideal channel state information means that the fading amplitudes $\rho_{k,n}$, k = 1, 2,..., K, are known at the receiver. In this case, assuming a soft Viterbi decoding it can be shown that the maximum-likelihood (ML) branch metrics are,

$$m(y_n, x_n; z_n) = -|y_n - x_n|^2 \quad (MRC) \tag{25}$$

$$m(y_n, x_n; z_n) = -\left|y_n - \sum_{k=1}^{K} \rho_{k,n} x_n\right|^2 \quad (EGC) \tag{26}$$

$$m(y_n, x_n; z_n) = -|y_n - \rho_{k,n} x_n|^2 \quad (SC)\,. \tag{27}$$

Therefore, the following expressions for the average bit error probability upper bound can be obtained (Appendix A),

$$P_b \le \sum_{N=L_e}^{\infty} \sum_{X_N} \sum_{\hat{X}_N} a(X_N, \hat{X}_N)\, p(X_N)\, \frac{1}{2} \prod_{n \in \eta} \left(1 + \frac{E_s}{4C_1 N_0} d_n^2\right)^{-K} \tag{28}$$

where C_1=1 or ε_K for MRC or EGC, respectively, and

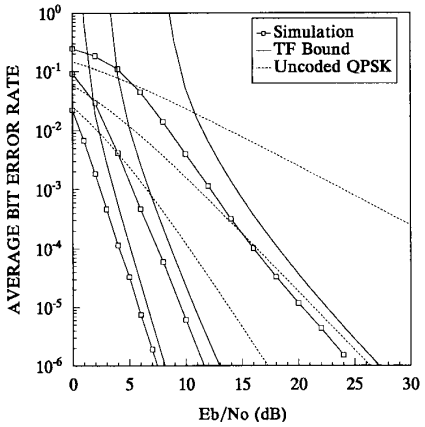

Fig. 2. BER *vs* E_b/N_0. Eight-state trellis code, ideal CSI, Predetection MRC K=1,2,3.

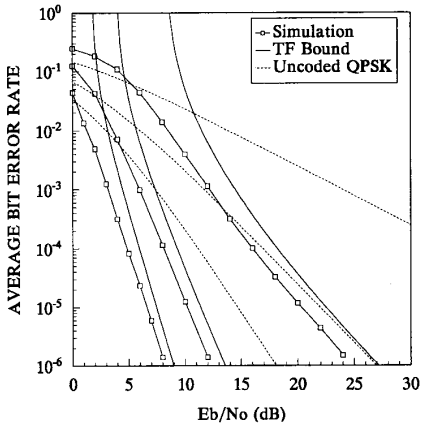

Fig. 3. BER *vs* E_b/N_0. Eight-state trellis code, ideal CSI, Predetection EGC K=1,2,3.

$$P_b \le \sum_{N=L_s}^{\infty} \sum_{X_N} \sum_{\hat{X}_N} a(X_N, \hat{X}_N) p(X_N) \cdot \frac{1}{2} \prod_{n=1}^{N} \sum_{i=0}^{K-1} \frac{(-1)^i K \binom{K-1}{i}}{1+i+\frac{E_s}{4N_0} d_n^2} \quad (SC) . \tag{29}$$

For large E_s/N_0, expressions (28)-(29) simplify to

$$P_b \le \sum_{N=L_s}^{\infty} \sum_{X_N} \sum_{\hat{X}_N} a(X_N, \hat{X}_N) p(X_N) \frac{1}{2} \prod_{n \in \eta} \left(\frac{E_s}{4C_1 N_0} d_n^2 \right)^{-K} \tag{30}$$

with $C_1=(K!)^{1/K}$ for SC. It is observed that the upper bound on P_b is dominated by the terms in the summation which have the smallest number of elements in η. These are referred as the shortest error event paths. Then, asymptotically, (30) can be simplified as

$$P_b \le \frac{1}{2k} C_2 \left(\frac{E_s}{4N_0} \right)^{-KL_s}, \tag{31}$$

where C_2 is a constant that depends on the type of diversity, on the distance structure of the code and is inversely proportional to $(\beta^2)^K$, with β^2 being the product of the normalized squared Euclidean distances along each of the shortest error event paths. Thus the code design criteria for minimizing BER after decoding is to maximize the length of the shortest error event paths and the product of the squared Euclidean distances along these paths. Furthermore, it is observed that the effect produced by the use of space diversity is similar (except constants) to that produced by the use of TCM. It is also interesting to notice that both factors, K and L_s, are multiplicative one with respect to the other.

Using the results of (28)-(29), transfer function (TF) upper bounds for the eight-state Ungerboeck's trellis-code in Rayleigh fading, with the number of diversity branches as parameter, are presented in Figs. 2-4[1]. Monte-Carlo simulation results are also provided and clearly indicate that the upper bounds become tighter as the number of diversity branches increases and thus the Rayleigh fading tends to be compensated for. The performance of QPSK reference systems

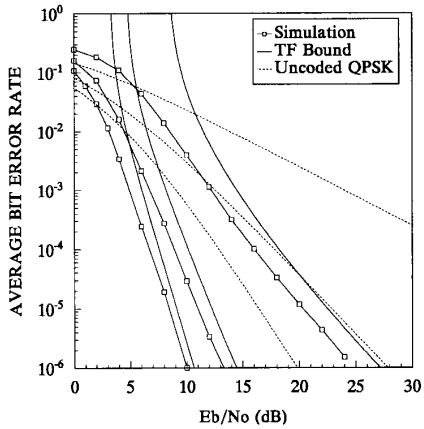

Fig. 4. BER *vs* E_b/N_0. Eight-state trellis code, ideal CSI, Predetection SC K=1,2,3.

is also presented. From these results, it can be observed that for average bit error rates of practical interest the trellis-coded modulation schemes perform better than uncoded schemes. For example, at an average BER of 10^{-3}, of interest in digital speech transmission, the eight-state trellis-coded systems, regardless of the predetection diversity scheme used at the receiver, offer coding gains relative to the corresponding uncoded QPSK reference systems of about 11.75 dB, 5.8 dB and 4.1 dB for K equal to 1, 2 and 3, respectively. Thus, it is obvious that relative coding gain lessens as the number of antennas in the diversity array is increased, therefore only diversity systems with up to three antennas will be considered of practical interest. It can be observed that for high signal to noise ratios, regardless of the system, predetection EGC and predetection SC are only, respectively, 0.62 dB and 1.5 dB inferior to predetection MRC for K=2. For K=3, predetection EGC and predetection SC are, respectively, 0.85 dB and 2.59 dB inferior to predetection MRC.

[1] For clarity reasons, curves are not labelled with the corresponding value of K. Anyway, they can be easily identified by its slope and because of its lower BER when increasing K.

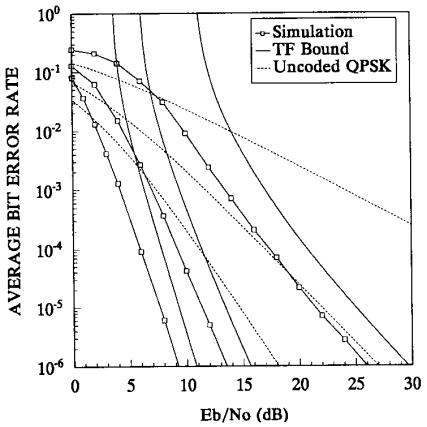

Fig. 5. BER *vs* E_b/N_0. Eight-state trellis code, no CSI, Predetection EGC K=1,2,3.

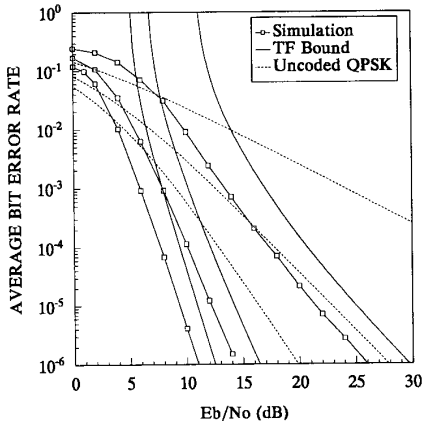

Fig. 6. BER *vs* E_b/N_0. Eight-state trellis code, no CSI, Predetection SC K=1,2,3.

2) No Channel State Information: When no CSI is provided the Gaussian metric takes the form

$$m(y_n, x_n) = -|y_n - x_n|^2 . \tag{32}$$

Thus, average bit error probability can be upperbounded as (Appendix B),

$$P_b \le \min_{\lambda \ge 0} \sum_{N=L_s}^{\infty} \sum_{X_N} \sum_{\hat{X}_N} a(X_N, \hat{X}_N) p(X_N) \cdot \frac{1}{2} \prod_{n \in \eta} \frac{2\epsilon_K^K \exp\left(K\lambda_0^2 d_n^2 \frac{E_s}{N_0}\right)}{(K-1)!} \cdot \int_0^{\infty} R_n^{2K-1} \exp\left[-\left(\epsilon_K R_n^2 + \lambda_0 \sqrt{K} d_n^2 \frac{E_s}{N_0} R_n\right)\right] dR_n \quad (EGC) \tag{33}$$

$$P_b \le \min_{\lambda \ge 0} \sum_{N=L_s}^{\infty} \sum_{X_N} \sum_{\hat{X}_N} a(X_N, \hat{X}_N) p(X_N) \cdot \frac{1}{2} \prod_{n \in \eta} 2K \exp\left(\lambda_0^2 d_n^2 \frac{E_s}{N_0}\right) \sum_{i=0}^{M-1} \binom{M-1}{i} (-1)^i \cdot \int_0^{\infty} R_n \exp\left[-\left((1+i)R_n^2 + \lambda_0 d_n^2 \frac{E_s}{N_0} R_n\right)\right] dR_n \quad (SC) . \tag{34}$$

These integrals are easily evaluated using iterative integration techniques, i.e.,

$$\mathbb{I}_k = \int_0^{\infty} x^k e^{-(ax^2+bx)} dx = \frac{1}{2a}\left[-x^{k-1} e^{-(ax^2+bx)} - b\mathbb{I}_{k-1} + (k-1)\mathbb{I}_{k-2}\right]_0^{\infty} \tag{35}$$

for k = 1, 2, 3, ... and with

$$\mathbb{I}_0 = \frac{1}{2}\sqrt{\frac{\pi}{a}} e^{b^2/4a} erfc \frac{b}{2\sqrt{a}} . \tag{36}$$

Using numerical techniques to perform minimization over the Chernoff parameter in (33) and (34), transfer function upper bounds for the eight-state trellis-code , with the number of diversity branches as parameter, are presented in Figs. 5 and 6. Monte-Carlo simulation results and the performance of QPSK reference systems are also shown. By comparing these results with the corresponding results for ideal CSI, a performance degradation of approximately 1.5 dB can be observed.

For large E_s/N_0 the asymptotic expansion of the complementary error function can be used, in which case the pairwise error probability reduces to

$$P(X_N \to \hat{X}_N) \le \min_{\lambda \ge 0} \frac{1}{2} \prod_{n \in \eta} \frac{2\epsilon_K^K (2K-1)!}{(K-1)!} \cdot \frac{\exp\left(K\lambda_0^2 d_n^2 \frac{E_s}{N_0}\right)}{\left(\lambda_0 \sqrt{K} d_n^2 \frac{E_s}{N_0}\right)^{2K}} \quad (EGC) \tag{37}$$

$$P(X_N \to \hat{X}_N) \le \min_{\lambda \ge 0} \frac{1}{2} \prod_{n \in \eta} (2K)! \frac{\exp\left(\lambda_0^2 d_n^2 \frac{E_s}{N_0}\right)}{\left(\lambda_0 d_n^2 \frac{E_s}{N_0}\right)^{2K}} \quad (SC). \tag{38}$$

These expressions can be optimized over the Chernoff parameter. Performing this optimization gives

$$(\lambda_0)_{opt} = \sqrt{L_\eta} \left(\frac{E_s}{N_0} \sum_{n \in \eta} d_n^2\right)^{-1/2} \tag{39}$$

where L_η is the length (diversity order) of the error event path corresponding to $\hat{X}_N$, i.e., the number of elements in η. Thus, λ_{opt} is a function of the distance structure of each individual error event, and not the ensemble. This could explain the fact that the transfer function bounds for the case of no CSI be approximately 1-1.5 dB weaker than the corresponding transfer function bounds for ideal CSI.

B. Postdetection diversity incoherent systems (TCM-MDPSK)

In this case, the nth element of the interleaved trellis coded symbol sequence X_N, namely x_n, is the phasor representation of the MPSK coded symbol $\Delta\phi_n$ assigned by the mapper in the nth transmission interval. It can be written as

$$x_n = e^{j\Delta\phi_n}. \tag{40}$$

Before transmission over the channel, the mapper output symbol sequence, X_N, is differentially encoded producing the sequence μ_N. In phasor notation, the MDPSK coded symbol in the nth transmission interval can be written as

$$\mu_n = \mu_{n-1}x_n = \sqrt{2E_s}\, e^{j(\phi_{n-1}+\Delta\phi_n)} = \sqrt{2E_s}\, e^{j\phi_n}. \tag{41}$$

and the transmitted bandpass signal is

$$\mu_T(t) = \mathbb{R}e\left\{\mu(t)\, e^{j\omega_c t}\right\} = \mathbb{R}e\left\{\sum_k \mu_k\, h_T(t-kT)\, e^{j\omega_c t}\right\}. \tag{42}$$

Assuming a K branch diversity system and the use of an ideal automatic frequency control (AFC), that is, a perfect compensation of frequency offsets between emitter and receiver local oscillators, the complex envelope of the received signal and the signal at the output of the reception filter in the kth receiver (k=1, 2, ..., K) can be expressed as

$$r_k(t) = \chi_k(t)\,\mu(t) + v_k(t) \tag{43}$$

and

$$w_k(t) = \chi_k(t)\sum_k \mu_k h(t-kT) + n_k(t) = \chi_k(t)\,\mu_f(t) + n_k(t), \tag{44}$$

respectively. In a postdetection diversity receiver, including the differential detection function [12], each branch input signal is multiplied by its delayed replica, with the time delay t_d=T for differential detection and lowpass filtered. Thus, the complex envelope of the resultant signal at the output of the lowpass filter is

$$g_k(t) = \chi_k(t)\chi_k^*(t-T)\mu_f(t)\mu_f^*(t-T) + \chi_k^*(t-T)\mu_f^*(t-T)n_k(t) + \chi_k(t)\,\mu_f(t)\,n_k^*(t-T) + n_k(t)\,n_k^*(t-T). \tag{45}$$

Assuming that the fading is slow varying enough that $\chi_k(t)\chi_k^*(t-T)\approx\rho_k^2(t)$ and that for high signal to noise ratios the last component of (45) can be neglected, then,

$$z(t) \propto \sum_{k=1}^{M}\left[\rho_k^2(t)\,\mu_f(t)\,\mu_f^*(t-T) + \chi_k^*(t)\,\mu_f^*(t-T)\,n_k(t) + \chi_k(t)\,\mu_f(t)\,n_k^*(t-T)\right] \quad (MRC). \tag{46}$$

This equation shows that the signal and noise contributions at the combiner output are both weighted by a factor equal to the absolute value of the fading. This weighting factor is that necessary to produce predetection MRC [1]. Hence, this can be termed postdetection MRC.

If a limiter giving unity amplitude is used in the feed-forward signal path of the postdetection diversity receiver [12], then, for high signal to noise ratios, the combiner output can be approximated by

$$z(t) \propto \frac{1}{\sqrt{2E_s}}\sum_{k=1}^{M}\left[\rho_k(t)\,\mu_f(t)\,\mu_f^*(t-T) + e^{-j\psi_k(t)}\,\mu_f^*(t-T)\,n_k(t) + e^{j\psi_k(t)}\,\mu_f(t)\,n_k^*(t-T)\right] \quad (EGC). \tag{47}$$

In this case, the weighting factor is unity for all branches and hence this can be termed postdetection EGC. Since this system can use mixers instead of multipliers, postdetection EGC can easily be built and is considered to be more practical.

The postdetection diversity receiver can also be used to implement a postdetection selection combining (SC) diversity scheme. Postdetection SC is the simplest system and selects the demodulator output associated to the branch having the largest input signal envelope, that is, the combiner output is given by

$$z(t) = w_k(t)\,w_k^*(t-T) \quad (SC). \tag{48}$$
$$|w_k(t)| > |w_q(t)|\ \forall\ q \neq k,\quad q \in [1,\ldots,K]$$

The combiner output is sent to the demodulator to obtain in-phase and quadrature channel outputs. After filtering, these signals are sampled by an A/D converter. Assuming a perfect clock recovery, the complex sample at the deinterleaver output, that is, the nth element of the output sequence Y_N corresponding to the input sequence X_N will be given by

$$y_n = \sum_{k=1}^{K} w_{k,n-1}^*\, w_{k,n} \quad (MRC) \tag{49}$$

$$y_n = \sum_{k=1}^{K} \frac{w_{k,n-1}^*\, w_{k,n}}{|w_{k,n}|} \quad (EGC) \tag{50}$$

$$y_n = w_{k,n-1}^*\, w_{k,n} \quad (SC). \tag{51}$$

Using these quantized symbols, the trellis decoder, implemented as a Viterbi algorithm with a metric depending upon whether or not channel state information (CSI) is provided, detects the transmitted sequence based on maximum likelihood estimation.

In the predetection diversity MRC coherent system, CSI is provided through the local signal $\chi_k^*(t)$ (see expression (18)) used in the detection process. Thus, comparing the system model for predetection MRC and postdetection MRC and SC diversity schemes, it can be noticed that in the last case a measure of CSI is provided by the delayed replica of the input signal. For the postdetection EGC scheme a measure of CSI could be obtained from envelope detection of the received signal. In all these cases, the optimum (maximum-likelihood) metric depends on the joint two-dimensional (amplitude and

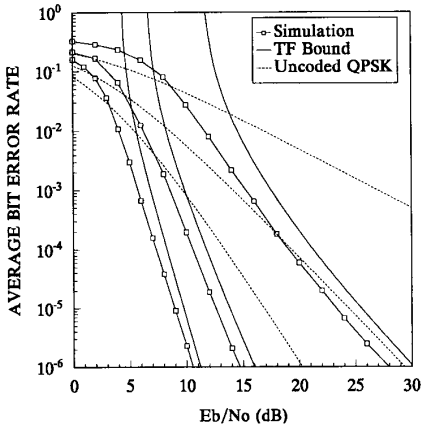

Fig. 7. BER *vs* E_b/N_0. Eight-state trellis code, Postdetection MRC K=1,2,3.

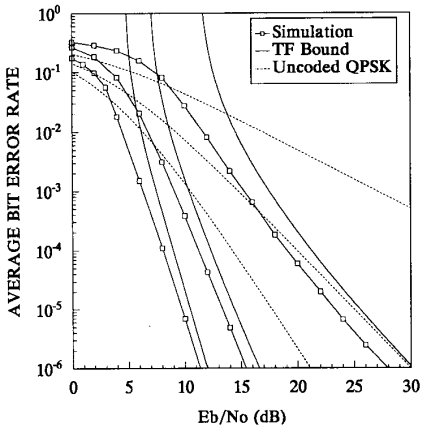

Fig. 8. BER *vs* E_b/N_0. Eight-state trellis code, Postdetection EGC K=1,2,3.

phase) statistics of a received sequence and is quite complicated to implement [4]. Assuming a soft Viterbi decoding based on the much simpler Gaussian metric [13], i.e,

$$m(y_n, x_n; z_n) = -|y_n - 2E_s x_n|^2 \quad (MRC) \tag{52}$$

$$m(y_n, x_n; z_n) = -\left|y_n - 2E_s \sum_{k=1}^{K} |w_{k,n}| x_n\right|^2 \quad (EGC) \tag{53}$$

$$m(y_n, x_n; z_n) = -|y_n - 2E_s x_n|^2 \quad (SC)\ , \tag{54}$$

the following expressions for the average bit error probability upper bound can be obtained (Appendix C),

$$P(X_N \to \hat{X}_N)$$

$$\le \min_{\lambda \ge 0} \frac{1}{2} \prod_{n \in \eta} \left[1 + d_n^2 \left(2\lambda_0 \frac{E_s}{N_0}(1 - 4\lambda_0) - (2\lambda_0)^2\right)\right]^{-K} \quad (MRC) \tag{55}$$

$$P(X_N \to \hat{X}_N) \le \min_{\lambda \ge 0} \frac{1}{2} \prod_{n \in \eta} \cdot \sum_{i=0}^{K-1} \frac{(-1)^i K \binom{K-1}{i}}{1 + i + d_n^2 \left(2\lambda_0 \frac{E_s}{N_0}(1 - 4\lambda_0) - (1+i)(2\lambda_0)^2\right)} \quad (SC). \tag{56}$$

Optimizing (55) over the Chernoff bound parameter we get,

$$P_b \le \sum_{N=L_s}^{\infty} \sum_{X_N} \sum_{\hat{X}_N} a(X_N, \hat{X}_N) p(X_N) \cdot \frac{1}{2} \prod_{n \in \eta} \left[\frac{1 - \gamma^2}{1 - \gamma^2 \left(1 - \frac{d_n^2}{4}\right)}\right]^K \quad (MRC) \tag{57}$$

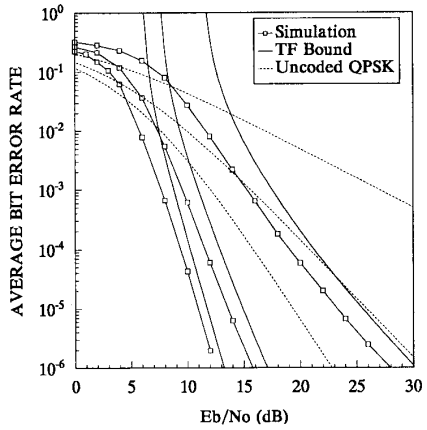

Fig. 9. BER *vs* E_b/N_0. Eight-state trellis code, Postdetection SC K=1,2,3.

where $\gamma = (E_s/N_0)/(1+(E_s/N_0))$. The result in (56) cannot be optimized over λ independent of the index n, and thus, for this case, we first must compute the average bit error probability and then optimize over the Chernoff parameter.

For the postdetection EGC scheme, evaluation of the expectation required in (C.6) is cumbersome. However, at signal-to-noise ratios of practical interest, the combiner output signal can be approximated by (47), and thus applying the same method used in the analysis of predetection diversity coherent systems with CSI, we get

$$P_b \le \sum_{N=L_s}^{\infty} \sum_{X_N} \sum_{\hat{X}_N} a(X_N, \hat{X}_N) p(X_N) \cdot \frac{1}{2} \prod_{n \in \eta} \left(1 + \frac{1}{\epsilon_K} \frac{E_s}{8N_0} d_n^2\right)^{-K} \quad (EGC)\ . \tag{58}$$

For large E_s/N_0, the average bit error probability bounds for postdetection diversity MRC and EGC TCM-MDPSK systems simplify to an expression which is identical to (30) except for

a scale factor of one half over the E_s/N_0 ratio. Thus, roughly speaking, we can conclude that the BER performance of postdetection diversity MRC and EGC differentially coherent systems with CSI and a Gaussian decoding metric is 3 dB poorer than that of the corresponding predetection diversity coherent systems with ideal (perfect) CSI and a Gaussian decoding metric. The numerical results in Figs. 7 and 8 may assist the reader in assessing the accuracy of this assertion. The asymptotic average BER for the postdetection diversity SC TCM-MDPSK scheme can be upper bounded by

$$P_b \le \min_{\lambda \ge 0} \sum_{N=L_s}^{\infty} \sum_{X_N} \sum_{\hat{X}_N} a(X_N, \hat{X}_N) p(X_N) \cdot \frac{1}{2} \prod_{n \in \eta} \frac{K! \left(1 - d_n^2 (2\lambda_0)^2\right)^{K-1}}{\left(d_n^2 2\lambda_0 \frac{E_s}{N_0} (1 - 4\lambda_0)\right)^K}. \tag{59}$$

The numerator of (59) has little effect on the optimization process, thus maximizing the denominator gives $(\lambda_0)_{opt} \simeq 1/8$. Although this is not the optimum value of λ_0 for (59), we use it nevertheless (resulting in a looser upper bound) to arrive at a result in a desirable form. Thus, substituting it in (59) we obtain

$$P_b \le \sum_{N=L_s}^{\infty} \sum_{X_N} \sum_{\hat{X}_N} a(X_N, \hat{X}_N) p(X_N) \frac{1}{2} \prod_{n \in \eta} \frac{K! \left(1 - \frac{d_n^2}{16}\right)^{K-1}}{\left(\frac{E_s}{8N_0} d_n^2\right)^K}. \tag{60}$$

The primary difference between this expression and that obtained for predetection diversity SC coherent systems is the manner in which it depends on both the distance structure of the trellis code and the number of antennas in the space diversity array. In fact, by considering only the shortest error event paths (which dominate the average BER performance at high SNR's) we conclude that, for K=2, the BER performance of eight-state postdetection diversity SC incoherent system 2.55 dB poorer than that of the corresponding predetection diversity coherent system. For K=3, the incoherent system differs from the coherent one in 2.40 dB for the eight-state trellis-code. This asymptotic tendency can be assessed by comparing theoretical upper bounds and Monte-Carlo simulation results presented in Fig. 9 with those shown in Fig. 4.

IV. Improved Upper Bound for MRC Schemes

The bounding procedures used in the previous section, although readily determined, produce a relatively weak upper bound, even at high signal-to-noise ratios. Therefore, it seems that there is still place for further improvement if more involved formulation is adopted. In this section we present a new asymptotically tight upper performance bound for predetection (PRE) and postdetection (POST) diversity MRC schemes, based on the exact calculation of the pairwise error probability. In the case of predetection diversity we assume perfect Channel Side Information.

Substituting (25) and (52) into (4) gives

$$f = \sum_{n=1}^{N} \sum_{k=1}^{K} C_3 U_{k,n}^{*T} F_n U_{k,n} \tag{61}$$

where C_3=1 or $2E_s$ for predetection and postdetection schemes, respectively, F_n is given by expression (C.4) and

$$U_{k,n} = \begin{cases} \begin{bmatrix} \chi_{k,n} \\ \chi_{k,n} x_n + n_{k,n} \end{bmatrix} & (PRE) \\ \begin{bmatrix} \chi_{k,n-1} x_{n-1} + n_{k,n-1} \\ \chi_{k,n} x_n + n_{k,n} \end{bmatrix} & (POST) \end{cases} \tag{62}$$

In a Rayleigh fading channel, $\chi_{k,n}$ and $n_{k,n}$ are zero-mean Gaussian distributed random variables and $U_{k,n}$ is a zero-mean Gaussian vector. Furthermore, assuming a perfect interleaving/deinterleaving process and an antenna spacing such that the individual signals are uncorrelated, $U_{k,n-1}$, $U_{k,n}$, $U_{k-1,n-1}$ and $U_{k-1,n}$ will be independent zero-mean Gaussian vectors and thus, f in (61) will be a double sum of independent quadratic forms of zero-mean Gaussian random variables. The pdf of f is not an elementary function but its characteristic function is given by [14, appendix 4B] as

$$G_f(t) = \prod_{n \in \eta} \prod_{k=1}^{K} \frac{1}{\det\left(I - jt2C_3 R_{k,n}^* F_n\right)} \tag{63}$$

where

$$E\left\{\exp\left(\hat{\lambda} U_{k,n}^{*T} F_n U_{k,n}\right) \mid x_n, \rho_{k,n}\right\} = \frac{\exp\left(-\hat{\lambda} E\left\{U_{k,n}^{*T}\right\} F_n \left(I + 2\hat{\lambda} R_{k,n}^* F_n\right)^{-1} E\left\{U_{k,n}\right\}\right)}{\det\left(I + 2\hat{\lambda} R_{k,n}^* F_n\right)}. \tag{64}$$

By solving the determinant in (63) we obtain

$$G_f(t) = \prod_{n \in \eta} \prod_{k=1}^{K} \frac{(t - t_{n1})^{-1} (t - t_{n2})^{-1}}{4E_s N_0 d_n^2} \quad (PRE) \tag{65}$$

$$G_f(t) = \prod_{n \in \eta} \prod_{k=1}^{K} \frac{(t - t_{n1})^{-1} (t - t_{n2})^{-1}}{16E_s^2 N_0^2 \left(2\frac{E_s}{N_0} + 1\right) d_n^2} \quad (POST) \tag{66}$$

where

$$t_{n1,n2} = -\frac{j}{4N_0} \left(1 \pm \sqrt{1 + \frac{4}{\frac{E_s}{N_0} d_n^2}}\right) \quad (PRE) \tag{67}$$

$$t_{n1,n2} = -\frac{j}{8N_0^2 \left(2\frac{E_s}{N_0} + 1\right)} \left(1 \pm \sqrt{1 + \frac{\left(2\frac{E_s}{N_0} + 1\right)}{\left(\frac{E_s}{2N_0}\right)^2 d_n^2}}\right) \quad (POST) \tag{68}$$

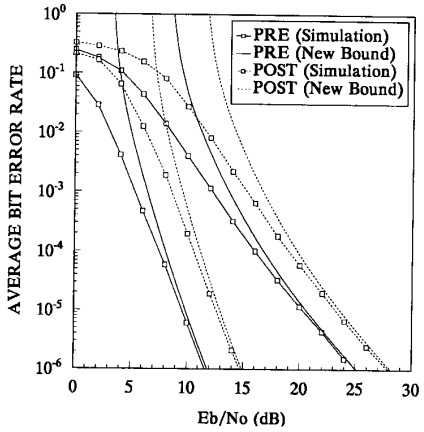

Fig. 10. BER *vs* E_b/N_0. Eight-state trellis code, Pre and Postdetection MRC K=1,2,3.

The pairwise error probability can be expressed in terms of $G_f(jt)$ as [14, appendix 4B]

$$P\left(X_N \to \hat{X}_N\right) = Pr\left(f \geq 0 \mid X_N\right) = \frac{-1}{2\pi j}\int_{-\infty+j\varepsilon}^{\infty+j\varepsilon} \frac{G_f(jt)}{t}\,dt \quad (69)$$

where ε is a small positive number. Substituting (65) and (66) in (69) and closing the path of integration with a semicircle of radius $R\to\infty$ we have that, except for a finite number of poles, the function $G_f(jt)/t$ is regular in the region bounded by the closed path. Thus, based on the theorem of residues from the theory of functions of a complex variable, the integral in (69) can be solved in closed form using the contour integration method.

This method, although mathematically simple, is not considered a practical approach for evaluating functions with a large number of poles of high order; so, we apply an upper bounding procedure similar to that proposed by McKay *et al.* [5]. First, m of the most dominant error events, in terms of asymptotic contribution to P_b, are selected from the code trellis. Their associated exact pairwise error probabilities are next calculated using the contour integration method. The pairwise error probability for all remaining error events is upper bounded by the weaker bounding procedures described in Section III. All these pairwise error probabilities are augmented with terms $Z^{a(xn,\hat{x}n)}$, summed, and finally, the average bit error probability upper bound is obtained by performing the differentiation indicated in (11). Obviously, the greater the number of error events considered in the set of "most dominant error events" the tighter the upper bound will be, but at the expense of increasing the complexity in finding the residues corresponding to the poles of the $G_f(jt)/t$ function.

In deriving this improved upper bound for the eight-state Ungerboeck's code in Rayleigh fading, error events having diversity two and three have been considered in the set of "most dominant error events". The obtained results have been plotted in Fig. 10. We observe that for low average bit error rates this upper bound, which is dominated by the pairwise error probabilities calculated using the contour integration method (the other error events have little effect in this region), achieves considerable improvement over the standard transfer function bounding techniques described in Section III. However, only marginal improvement is achievable at high average bit error rates, since the peak singularity occurring in the transfer function bounding techniques dominates the bound in this region.

V. Conclusions

In this paper, the bit error rate (BER) performance of predetection diversity trellis coded multilevel phase shift keying (TCM-MPSK) and postdetection diversity trellis coded multilevel differential phase shift keying (TCM-MDPSK), transmitted over a Rayleigh fading channel has been presented. Novel analytical upper bounds using the transfer function bounding technique have been obtained and illustrated by several numerical examples. A new asymptotically tight upper bound for the Maximal Ratio Combining (MRC) diversity schemes has been also derived. In order to analyze practical TCM schemes (four or more states), only trellis codes holding uniform error property (UEP) and uniform distance property (UDP) have been considered, enabling the encoder transfer function to be obtained from a modified state transition diagram, having no more states than the encoder itself. Monte-Carlo simulation results, which are more indicative of the exact system performance, as well as the BER performance of QPSK and QDPSK reference systems have been also given. Theoretical and simulation results have shown that a substantial reduction in the average BER due to Gaussian noise can be obtained in a Rayleigh fading environment if space diversity is used in conjunction with trellis coding techniques. BER performance analysis has also shown that, regardless of the number of antennas in the diversity array, postdetection diversity systems using MRC, EGC and SC have a performance degradation of at most 3 dB, compared to the corresponding predetection diversity systems.

Appendix A

Substituting (25), (26) and (27) into (4) gives

$$f = \sum_{n=1}^{N}\sum_{k=1}^{K}\left(-\rho_{k,n}^2\left|\hat{x}_n - x_n\right|^2 + 2\mathbf{Re}\left\{\chi_{k,n}^{*} n_{k,n}\left(\hat{x}_n - x_n\right)^{*}\right\}\right) \quad (MRC) \quad (A.1)$$

$$f = \sum_{n=1}^{N}\sum_{k=1}^{K}\sum_{m=1}^{K}\left(-\rho_{k,n}\rho_{m,n}\left|\hat{x}_n - x_n\right|^2 + \rho_{m,n} n_{k,n}\left(\hat{x}_n - x_n\right)^{*} + \rho_{k,n} n_{m,n}^{*}\left(\hat{x}_n - x_n\right)\right) \quad (EGC) \quad (A.2)$$

$$f = \sum_{n=1}^{N}\left(-\rho_{k,n}^2\left|\hat{x}_n - x_n\right|^2 + 2\mathbf{Re}\left\{\rho_{k,n} n_{k,n}\left(\hat{x}_n - x_n\right)^{*}\right\}\right) \quad (SC) \quad (A.3)$$

By conditioning on the fading, clearly f is a Gaussian random variable with mean μ and variance σ^2 which can be shown to be given by

$$\mu = \begin{cases} -2E_s \sum_{n=1}^{N} \sum_{k=1}^{K} \rho_{k,n}^2 d_n^2 & (MRC) \\ -2E_s \sum_{n=1}^{N} \left(\sum_{k=1}^{K} \rho_{k,n} \right)^2 d_n^2 & (EGC) \\ -2E_s \sum_{n=1}^{N} \rho_{k,n}^2 d_n^2 & (SC) \end{cases} \quad (A.4)$$

$$\sigma^2 = \begin{cases} 8E_s N_0 \sum_{n=1}^{N} \sum_{k=1}^{K} \rho_{k,n}^2 d_n^2 & (MRC) \\ 8KE_s N_0 \sum_{n=1}^{N} \left(\sum_{k=1}^{K} \rho_{k,n} \right)^2 d_n^2 & (EGC) \\ 8E_s N_0 \sum_{n=1}^{N} \rho_{k,n}^2 d_n^2 & (SC) \end{cases} \quad (A.5)$$

where d_n^2 is the normalized squared Euclidean distance defined as

$$d_n^2 \doteq \frac{|x_n - \hat{x}_n|^2}{2E_s} = 2\left[1 - \cos\left(\hat{\phi}_n - \phi_n\right)\right]. \quad (A.6)$$

Thus, the conditional exact pairwise error probability will be given by

$$P\left(X_N \to \hat{X}_N \mid \rho_{1,N}, \ldots, \rho_{K,N}\right) = \frac{1}{2} erfc\left(\frac{\mu}{\sqrt{2}\,\sigma}\right). \quad (A.7)$$

By defining the random variable

$$R_n = \begin{cases} \sqrt{\sum_{k=1}^{K} \rho_{k,n}^2} & (MRC) \\ \frac{1}{\sqrt{K}} \sum_{k=1}^{K} \rho_{k,n} & (EGC) \\ \max\left(\rho_{1,n}, \rho_{2,n}, \ldots, \rho_{K,n}\right) & (SC) \end{cases} \quad (A.8)$$

and conditioning the pairwise error probability on $\boldsymbol{R}_N$ we get

$$P\left(X_N \to \hat{X}_N \mid \boldsymbol{R}_N\right) = \frac{1}{2} erfc\left(\sqrt{\frac{E_s}{4N_0} \sum_{n=1}^{N} R_n^2 d_n^2}\right). \quad (A.9)$$

In order to evaluate the average bit error probability, we must first evaluate unconditional pairwise error probabilities by averaging (A.9) over the pdf of R_N. This would require the evaluation of multiple integrals and could be achieved using numerical techniques, but is not considered a practical approach. In order to overcome this problem, the inequality $erfc\ x \le exp(-x^2)$ can be used to bound (A.9) in product form as

$$P\left(X_N \to \hat{X}_N \mid \boldsymbol{R}_N\right) \le \frac{1}{2} \prod_{n \in \eta} \exp\left(-\frac{E_s}{4N_0} R_n^2 d_n^2\right) \quad (A.10)$$

where η is the set of all n such that $x_n \neq \hat{x}_n$. Thus, the unconditional pairwise error probability upper bound is obtained by averaging (A.10) over the pdf of $\boldsymbol{R}_N$. Since we have assumed that the interleaving/deinterleaving makes the R_n's independent, then the average over $\boldsymbol{R}_N$ can be computed as the product of the averages. Furthermore, since all $R_{k,n}$ are independent Rayleigh r.v.'s, the pdf of R_n can be expressed as

$$p(R_n) = \begin{cases} K \frac{R_n}{\sigma_R^2} \exp\left(-\frac{R_n^2}{2\sigma_R^2}\right)\left[1 - \exp\left(-\frac{R_n^2}{2\sigma_R^2}\right)\right]^{K-1} & (SC) \\ \frac{1}{(K-1)!} \frac{R_n}{\sigma_R^2} \left(\frac{R_n^2}{2\sigma_R^2}\right)^{K-1} \exp\left(-\frac{R_n^2}{2\sigma_R^2}\right) & (MRC). \end{cases} \quad (A.11)$$

For EGC, a good approximation can be obtained using the pdf of MRC, by replacing σ_R^2 by σ_R^2/ε_K [2] where $\varepsilon_K = K/\{(2K-1)!!\}^{1/K}$. Averaging (A.10) over (A.11) leads to expressions (28)-(29).

APPENDIX B

Substituting (32) into (4) gives

$$f = \sum_{n=1}^{N} \sum_{k=1}^{K} \left(-\rho_{k,n} |\hat{x}_n - x_n|^2 + 2\mathbf{Re}\left\{ e^{-j\psi_{k,n}} n_{k,n} (\hat{x}_n - x_n)^* \right\} \right) \quad (EGC) \quad (B.1)$$

$$f = \sum_{n=1}^{N} \left(-\rho_{k,n} |\hat{x}_n - x_n|^2 + 2\mathbf{Re}\left\{ e^{-j\psi_{k,n}} n_{k,n} (\hat{x}_n - x_n)^* \right\} \right) \quad (SC). \quad (B.2)$$

By conditioning on the fading, f becomes a Gaussian random variable with mean μ and variance σ^2 given by

$$\mu = \begin{cases} -2E_s \sum_{n=1}^{N} \sum_{k=1}^{K} \rho_{k,n} d_n^2 & (EGC) \\ -2E_s \sum_{n=1}^{N} \rho_{k,n} d_n^2 & (SC) \end{cases} \quad (B.3)$$

$$\sigma^2 = \begin{cases} 8KE_s N_0 \sum_{n=1}^{N} d_n^2 & (EGC) \\ 8E_s N_0 \sum_{n=1}^{N} d_n^2 & (SC). \end{cases} \quad (B.4)$$

Thus, using expression (A.8), the conditional exact pairwise error probability is given by

$$P\left(X_N \to \hat{X}_N \mid \boldsymbol{R}_N\right) = \frac{1}{2}\, erfc\left(\frac{2E_s \sum_{n=1}^{N} R_n d_n^2}{\sqrt{16 E_s N_0 \sum_{n=1}^{N} d_n^2}}\right). \quad \text{(B.5)}$$

In order to express the pairwise error probability in product form we can upperbound (B.5) by using the Chernoff bound [3], [8]. In this case, the conditional pairwise error probability can be bounded as

$$P\left(X_N \to \hat{X}_N \mid \boldsymbol{R}_N\right) \le \min_{\lambda \ge 0} \frac{1}{2} \prod_{n \in \eta} \prod_{k=1}^{K} \exp\left[-\lambda \rho_{k,n} 2E_s d_n^2\right] \quad (EGC)$$
$$\cdot E\left\{\exp\left[2\lambda \mathbb{R}e\left\{e^{-j\psi_{k,n}} n_{k,n}\left(\hat{x}_n - x_n\right)^*\right\}\right] \mid x_n, \rho_{k,n}\right\} \quad \text{(B.6)}$$

$$P\left(X_N \to \hat{X}_N \mid \boldsymbol{R}_N\right) \le \min_{\lambda \ge 0} \frac{1}{2} \prod_{n \in \eta} \exp\left[-\lambda \rho_{k,n} 2E_s d_n^2\right] \quad (SC)$$
$$\cdot E\left\{\exp\left[2\lambda \mathbb{R}e\left\{e^{-j\psi_{k,n}} n_{k,n}\left(\hat{x}_n - x_n\right)^*\right\}\right] \mid x_n\right\} \quad \text{(B.7)}$$

where the E operator denotes statistical expectation over the additive noise and λ is the Chernoff parameter to be optimized. Evaluating the expectation required in (B.6) and (B.7) yields

$$P\left(X_N \to \hat{X}_N \mid \boldsymbol{R}_N\right) \le \min_{\lambda \ge 0} \frac{1}{2} \prod_{n \in \eta} D^{c^2\left(x_n, \hat{x}_n \mid \boldsymbol{R}_n\right)} \quad \text{(B.8)}$$

D being the Bhattacharyya distance defined as $D = \exp(-E_s/4N_0)$, and

$$c^2\left(x_n, \hat{x}_n \mid \boldsymbol{R}_n\right) = 4\lambda_0 d_n^2\left(\sqrt{K}\boldsymbol{R}_n - K\lambda_0\right) \quad (EGC) \quad \text{(B.9)}$$

$$c^2\left(x_n, \hat{x}_n \mid \boldsymbol{R}_n\right) = 4\lambda_0 d_n^2\left(\boldsymbol{R}_n - \lambda_0\right) \quad (SC) \quad \text{(B.10)}$$

where $\lambda_0 = 2\lambda N_0$. Expression (B.8) cannot be optimized over λ independent of the index n. Thus, we must first average over the fading distribution. By using (A.11) we obtain (33) and (34).

APPENDIX C

Substituting (52), (53) and (54) into (4) and taking into account that $|x_n| = |\hat{x}_n|$, we obtain

$$f = \sum_{n=1}^{N} \sum_{k=1}^{K} 2E_s U_{k,n}^{*T} F_n U_{k,n} \quad (MRC) \quad \text{(C.1)}$$

$$f = \sum_{n=1}^{N} \sum_{k=1}^{K} \sum_{m=1}^{K} 2E_s \frac{|w_{m,n}|}{|w_{k,n}|} U_{k,n}^{*T} F_n U_{k,n} \quad (EGC) \quad \text{(C.2)}$$

$$f = \sum_{n=1}^{N} 2E_s U_{k,n}^{*T} F_n U_{k,n} \quad (SC) \quad \text{(C.3)}$$

where superscripts * and T denote complex conjugate and matrix transpose and

$$F_n = \begin{bmatrix} 0 & \left(\hat{x}_n - x_n\right)^* \\ \left(\hat{x}_n - x_n\right) & 0 \end{bmatrix}, \quad U_{k,n} = \begin{bmatrix} w_{k,n-1} \\ w_{k,n} \end{bmatrix}. \quad \text{(C.4)}$$

Then, conditioning on the fading, the pairwise error probability has the Chernoff upper bound

$$P\left(X_N \to \hat{X}_N \mid \boldsymbol{R}_N\right) \le \min_{\lambda \ge 0} \frac{1}{2} \prod_{n \in \eta} \prod_{k=1}^{K} \quad (MRC) \quad \text{(C.5)}$$
$$\cdot E\left\{\exp\left(2E_s \lambda U_{k,n}^{*T} F_n U_{k,n} \mid x_n, \rho_{k,n}\right)\right\}$$

$$P\left(X_N \to \hat{X}_N \mid \boldsymbol{R}_N\right) \le \min_{\lambda \ge 0} \frac{1}{2} \prod_{n \in \eta} \prod_{k=1}^{K} \prod_{m=1}^{K} \quad (EGC)$$
$$\cdot E\left\{\exp\left(2E_s \lambda \frac{|w_{m,n}|}{|w_{k,n}|} U_{k,n}^{*T} F_n U_{k,n} \mid x_n, \rho_{k,n}, \rho_{m,n}\right)\right\} \quad \text{(C.6)}$$

$$P\left(X_N \to \hat{X}_N \mid \boldsymbol{R}_N\right) \le \min_{\lambda \ge 0} \frac{1}{2} \prod_{n \in \eta} \quad (SC) \quad \text{(C.7)}$$
$$\cdot E\left\{\exp\left(2E_s \lambda U_{k,n}^{*T} F_n U_{k,n} \mid x_n, \rho_{k,n}\right)\right\}$$

Manipulating these expressions [14], (C.5) and (C.7) lead to

$$P\left(X_N \to \hat{X}_N \mid \boldsymbol{R}_N\right) \le \min_{\lambda \ge 0} \frac{1}{2} \prod_{n \in \eta} \zeta^K \exp\left(-\xi \boldsymbol{R}_n^2\right) \quad (MRC) \quad \text{(C.8)}$$

$$P\left(X_N \to \hat{X}_N \mid \boldsymbol{R}_N\right) \le \min_{\lambda \ge 0} \frac{1}{2} \prod_{n \in \eta} \zeta \exp\left(-\xi \boldsymbol{R}_n^2\right) \quad (SC) \quad \text{(C.9)}$$

with

$$\zeta = \frac{1}{1 - (2\lambda_0)^2 d_n^2} \quad ; \quad \xi = \frac{2\lambda_0 \frac{E_s}{N_0} d_n^2 (1 - 4\lambda_0)}{1 - (2\lambda_0)^2 d_n^2}. \quad \text{(C.10)}$$

where $\lambda_0 = \hat{\lambda} N_0$ and $d_n^2 = |\hat{x}_n - x_n|^2$. Averaging each term in the products of (C.8) and (C.9) over the corresponding pdf's in (A.11) leads to expressions (55) and (56).

REFERENCES

[1] D.G. Brennan, "Linear diversity combining techniques", *Proc. IRE*, 47, pp. 1075-1102, 1959.

[2] W. C. Jakes, Jr., *Microwave Mobile Communications*. New York: Wiley, 1974.

[3] D. Divsalar and M. K. Simon, "Trellis coded modulation for 4800-9600 bits/s transmission over a fading mobile satellite channel", *IEEE Journal Sel. Areas Commun.*, vol. SAC-5, pp. 162-175, 1987.

[4] M. K. Simon and D. Divsalar, "The performance of trellis coded multilevel DPSK on a fading mobile satellite channel", *IEEE Trans. Vehic. Tech.*, vol. 37, pp. 78-91, 1988.

[5] R. G. McKay, P. J. McLane and E. Biglieri, "Error bounds for trellis-coded MPSK on a fading mobile satellite channel", *IEEE Trans. Commun.*, vol. 39, pp. 1750-1761, 1991.

[6] J. Huang and L. L. Campbell, "Trellis coded MDPSK in correlated and shadowed rician fading channels", *IEEE Trans. Vehic. Tech.*, vol. 40, pp. 786-797, 1991.

[7] G. Ungerboeck, "Channel coding with multilevel/phase signals", *IEEE Trans. Inf. Theory*, vol. IT-28, pp. 56-66, 1982.

[8] M. K. Simon, J. K. Omura, R. A. Scholtz and B. K. Levitt, *Spread Spectrum Communications*, vol. 1. Rockville, MD: Computer Science Press, 1985.

[9] E. Biglieri, "High-level modulation and coding for nonlinear satellite channels", *IEEE Trans. Commun.*, vol. COM-32, pp. 616-626, 1984.

[10] E. Biglieri and P. J. McLane, "Uniform distance and error probability properties of TCM schemes", *IEEE Trans. Commun.*, vol. 39, pp. 41-53, 1991.

[11] A. J. Viterbi and J. K. Omura, *Principles of Digital Communication and Coding*. McGraw-Hill, 1979.

[12] J.D. Parsons and J.G. Gardiner, *Mobile Communication Systems*. USA:Halsted Press,1989.

[13] D.A. Johnston and S.K. Jones, "Spectrally efficient communication via fading channels using coded multilevel DPSK", *IEEE Trans. Commun.*, vol. COM-29, pp. 276-284, 1981.

[14] J.G. Proakis, *Digital Communications (2nd ed.)*. Singapore: McGraw Hill Book Co., 1989.

Guillem Femenias (M'91) was born in Petra, Spain, on August 20, 1963. He received the Engineer and Doctor Engineer degrees in telecommunication engineering from the Universitat Politècnica de Catalunya (UPC), Spain, in 1987 and 1991, respectively.

In 1987 he joined the Escola Tècnica Superior d'Enginyers de Telecomunicació de Barcelona, Spain, where he became Associate Professor in 1990. Now he is with the Departament de Ciències Matemàtiques i Informàtica, Universitat de les Illes Balears (UIB), Spain. He has been working in the field of digital radio communications, both fixed radio relay and mobile communications. His main research interests lie in the area of communication theory with particular emphasis on trellis coded modulation and personal, indoor and mobile radio communication systems. He is actively participating in the COST231 and RACE European research programs.

Ramón Agustí (M'78) was born in Riba-roja d'Ebre, Spain, on August 15, 1951. He received the Engineer of Telecommunications degree from the Universidad Politécnica de Madrid, Spain, in 1973, and the Ph. D. degree from the Universitat Politècnica de Catalunya, Spain, 1978.

In 1973, he joined the Escola Tècnica Superior d'Enginyers de Telecomunicació de Barcelona, Spain, where he became Full Professor in 1987. He has been working in the field of digital communications with particular emphasis on digital radio, both fixed radio relay and mobile communications. He has also been concerned with the performance analysis and development of frequency-hopped spread-spectrum systems. He is participating in the COST 231 and RACE European research programs. His research interests are in the area of communications theory with current emphasis on spread-spectrum systems, digital radio, and trellis coded modulation.